COHERENT DEMODULATION FOR ORTHOGONAL SIDEBAND AND CARRIER TRACKING

Sergei Udalov
Axiomatix
9841 Airport Blvd. , Ste 912
Los Angeles, California 90045

Summary - A demodulation technique which permits simultaneous coherent and orthogonal tracking of a suppressed carrier and of the associated sidebands is described. The performance of a demodulator based on such a technique is defined for a general case and for a specific case of two-channel FM multiplexing. Experimental data supporting the analysis of the FM multiplexing mode of the demodulator is presented and discussed.

Introduction - In recent years, the phase-locked loop (PLL) has found a number of successful applications in many aspects of communication engineering. It has been used as a threshold-extending coherent tracking device for doppler-shifted RF signals, as a frequency stabilizing element for high power crystal-controlled microwave RF generators, and as an efficient demodulator for frequency modulated (FM) signals. In all of these applications, the salient feature of the PLL, namely the coherent tracking of an input signal, plays the dominant role in determining the performance of a particular equipment.

The versatility inherent in a phase-locked loop configuration does not limit its application to those which involve coherent tracking of a single signal. As demonstrated in this paper, implementation configurations involving simultaneous phase-locked tracking of more than one signal are also possible. A demodulator configuration which provides for simultaneous and orthogonal coherent tracking of modulation sidebands and of the suppressed carrier is described and analyzed. One specific application of the orthogonal demodulator described in this paper involves de-multiplexing of two independent baseband channels. Modulation/demodulation orthogonality in this particular case is achieved by letting one baseband signal deviate the frequency of a subcarrier which in turn is impressed as double sideband (DSB) amplitude modulation on a carrier whose frequency is simultaneously deviated by the second baseband signal. The interesting feature of the phase-lock loop de-multiplexer described here is that it extracts the frequency modulation information of both the carrier and the subcarrier from the two groups of sidebands, the upper and the lower, and thus it allows for carrier suppression at the transmitter with consequent economy of RF power. Because both the multiplexing and the de-multiplexing

The author is with Axiomatix, Las Angeles, California

processes utilize the intrinsic orthogonality of the frequency and amplitude-modulated signals, no additional signal power is required for transmission of a second channel, provided that the phase-lock loops which perform the signal separation at the receiving end operate above threshold. On the other hand, once the signal-to-noise ratio in both loops falls below a certain critical value, a penalty paid for multiplexing manifests itself as a loss in output signal-to-noise ratio in each channel. The maximum penalty is paid at signal-to-noise ratios corresponding to the PLL threshold. Under these conditions the maximum penalty of 3 dB in power must be paid for doubling the number of baseband channels.

Basic Coherent Demodulator - The coherent orthogonal demodulator described in this paper evolves from the double sideband synchronous detector [1] which has become widely known under the name of a Costas loop or a Costas demodulator. The unique feature of the Costas demodulator is that it utilizes the sidebands to reconstruct the carrier of a double sideband suppressed carrier modulated signal. The behavior of the Costas demodulator is well documented in the open literature [2], with particular emphasis on the recovery of digital data modulation. Consequently, only a brief review of the fundamental operation of this demodulator is presented here.

Figure 1 shows the block diagram of a generic Costas demodulator. The input to the demodulator is a double sideband suppressed carrier amplitude-modulated by a sinusoid of frequency ω_a . As indicated in the block diagram, the input to the demodulator is applied simultaneously to “In-phase” and “Quadrature” detectors. When the demodulator is in lock, i.e., the carrier error is small, the in-phase detector recovers the amplitude modulation of the DSSCM, and the quadrature detector recovers the carrier tracking error. The amplitude modulation, which is riding on the carrier error signal developed by the quadrature detector, is removed by the carrier tracking error rectifier which is commonly referred to as the “third multiplier” of the Costas loop. For small values of α, the approximation $\sin \alpha \simeq \alpha$ provides for linear phase tracking of the suppressed carrier. Hence, it must be pointed out that because of the factor of 2 in the $\sin 2\alpha$ term, the Costas loop in the noiseless case can track the phase of the reconstructed carrier only over the range of ±45 degrees, while the conventional phase-lock loop can track the carrier, at least in principle, up to ±90 degrees. Another peculiarity of the Costas loop demodulator is that the reinsertion of the suppressed carrier provides an intrinsic ambiguity of 0° or 180°. Thus the polarity of the received amplitude information also includes this ambiguity.

For demodulation of conventional suppressed-carrier amplitude-modulated signal, the carrier tracking loop is used only to provide coherent reinsertion of the suppressed carrier and for tracking the slow changes in the carrier frequency such as may result from a doppler shift. The carrier modulation signal $\cos \omega_a t$ can represent either a single frequency of a baseband signal or, as in the case considered here, a subcarrier which in turn is modulated in one form or another. In a conventional Costas demodulator, the passband of

the modulation filters, also known as arm filters, should extend from DC to the highest frequency of modulation or be centered around the subcarrier frequency. In both cases, however, it must be kept in mind that the arm filters are components of the tracking loop and, therefore, their effect on carrier tracking cannot be neglected [3]. Furthermore, if the subcarrier is modulated, the bandwidth of the arm filters must be sufficiently broad to pass all significant sidebands in excess of the bandwidth of the subcarrier modulation signal. Such conditions degrade the performance of the carrier tracking loop, particularly, when the signal-to-noise ratios within the modulation filter bandwidth are low. Furthermore, since the carrier tracking is a necessary condition for the recovery of the subcarrier, the degradation of carrier loop's performance results also in a degradation in the performance of the entire circuit. The technique for providing optimum carrier tracking regardless of the bandwidth needed to pass the sidebands of a modulated subcarrier will now be described.

Coherent Orthoqonal Demodulator - The conventional Costas detector described thus far can track coherently the frequency and phase of the carrier, but it has no provisions for optimum recovery of the subcarrier signal and its modulation, if present. A logical first step for achieving such optimal recovery of a subcarrier would be to provide a coherent, phase-locked tracking demodulator for the subcarrier. Such a demodulator, when connected to the output of the I-channel, would recover in an optimum fashion the amplitude, the phase, or the frequency modulation from the subcarrier. Such an "external loop" demodulator would not provide, however, the means for reducing the bandwidth of the arm filters and, therefore, would not improve the carrier tracking properties of the conventional Costas demodulator.

To make the subcarrier demodulator loop aid the carrier tracking, the sideband demodulator must be properly coupled to the carrier tracking loop. Specifically, if the VCO output signal of the subcarrier tracking loop is substituted for the I-channel arm filter output signal, the noise bandwidth of the subcarrier tracking demodulator replaces the noise bandwidth of the arm filters. Because the noise bandwidth of the subcarrier tracking loop is generally much narrower than the noise bandwidth of the arm filters, the carrier tracking capabilities of the entire demodulator are improved. It is this interconnection of the carrier and the subcarrier tracking loops that distinguishes the coherent orthogonal demodulator described here from a conventional Costas loop.

The operating principle, and specifically the orthogonality of such a demodulator, can be understood best by considering the idealized block diagram of Figure 2. The block diagram shown can be functionally subdivided into three subunits. These are: (1) the carrier tracking loop, (2) the sideband tracking loop, and (3) the cross-coupling circuitry. Note that except for the differences in operating frequencies, the carrier and the subcarrier loops are identical. The elements comprising these loops are: an error detector, a low-pass filter, and a voltage-controlled oscillator (VCO). The cross-coupling circuitry consists of

the “in-phase” carrier and subcarrier detectors and the 90 degree phase shifters. The analytical expressions presented below explain the operation, in a noiseless case, of the orthogonal demodulator.

Assume that the input to the demodulator is a double-sideband, suppressed carrier signal of the form:

$$e_{in} = \sqrt{2S} \cos \omega_c t \cos \omega_s t \quad (1)$$

where

S = average received signal power
ω_c = carrier frequency
ω_s = subcarrier frequency

After carrying out several straightforward trigonometric manipulations and taking into account the effects of the low-pass filters, one can show that the carrier and the subcarrier tracking errors are, respectively [4]

$$\text{Carrier tracking error} = e_c = S K_2 K_4 \cos \theta \sin \alpha \quad (2)$$

$$\text{Subcarrier tracking error} = e_s = S K_1 K_3 \cos \alpha \sin \theta \quad (3)$$

Equations (2) and (3) demonstrate the orthogonality of the carrier and the subcarrier loops. Specifically, they imply that when the tracking errors in both loops are small, so that $\cos \theta \approx \cos \alpha, \approx 1$, the cross-coupling between the two loops is negligible despite the fact that the carrier VCO signal is used to recover the subcarrier tracking signal and vice versa. Furthermore, these equations indicate that the cross-coupling is defined by a cosine function, which is a relatively flat function for a considerable range of small errors.

Noise and Threshold Performance - So far the operation of the orthogonal demodulator was described without considering -quantitatively the effects of the noise and the modulation tracking errors, the latter being present when either loop is used as a frequency tracker. Now, the effect of these errors on the demodulator’s threshold performance will be analyzed. Specifically, it will be shown that as the error in each loop increases as a result of a lower input signal-to-noise ratio, the cross-coupling between the loops begins to affect the performance of each loop. Consequently, the signal-to-noise ratio in each of the cross-coupled loops reaches some arbitrary minimum threshold value sooner than for the case of a single phase-lock loop demodulator of the same noise bandwidth and with an identical input signal-to-noise ratio. However, as is shown below, the maximum degradation which may exist due to cross-coupling is 3 dB as compared to an identical single-loop, phase-lock demodulator.

The analysis used here constitutes an extension of the quasi-linearization analysis and the threshold criterion estimation for phase-lock tracking and demodulation and includes the effect of cross-coupling between the carrier and the subcarrier loops.

Quasi-linearization is an analytical method for defining the equivalent gain for a nonlinear device in terms of the statistical parameters of signals at the input to the device [5]. This method has been applied successfully to the analysis of the threshold behavior of a single loop phase-lock demodulator [6,7]. In this paper the quasi-linearization method is extended to the analysis of an orthogonal double loop demodulator. To simplify the analytical task it is assumed that both the noise and the modulation tracking error statistics are Gaussian-distributed. The modulation tracking error may be present in both the carrier and the subcarrier loops due to either an intentional (information) or an unintentional (frequency jitter) signal.

The first step in the analysis is to write the expression for the equivalent loop gain

$$K_{eq} = \int_{-\infty}^{\infty} g(\epsilon)\, P(\epsilon)\, d\epsilon \tag{4}$$

where $P(\epsilon)$, the probability distribution for the phase error, is a Gaussian distribution and $g(\epsilon)$ is the gain function of the nonlinear element. For a single phase-locked loop the gain function of the nonlinear element is the derivative of the error function. Thus,

$$g(\epsilon) = f'(\epsilon) = \frac{d}{d\epsilon}(\sin \epsilon) = \cos \epsilon \tag{5}$$

However, the demodulator described in this paper has two multipliers in each loop, the effect of each multiplier being described by a sine and a cosine term, respectively. Physically, this means that the gain of either loop is determined not only by the phase error within a given loop but also by the phase error in the companion loop.

Therefore, to find an expression for an equivalent gain of a carrier tracking loop one must evaluate the integral in Equation (4) over all possible errors of the carrier, as well as

$$K_{eq}\ (\text{carrier}) = \frac{S\, K_2\, K_4}{2\pi\sigma_\theta\sigma_\alpha} \int_{-\infty}^{\infty} \int_{-\infty}^{\infty} \cos\theta \cos\alpha \exp\left\{-\left(\frac{\theta^2}{2\sigma_\theta^2} + \frac{\alpha^2}{2\sigma_\alpha^2}\right)\right\} d\theta\, d\alpha \tag{6}$$

where as defined earlier in text and by Figure 2

- K_2 = gain constant of balanced modulator BM_2
- K_4 = gain constant of balanced modulator BM_4
- α = tracking error in the carrier loop
- θ = tracking error in the subcarrier loop
- σ_α = rms value of the phase error within the carrier loop
- σ_θ = rms value of the phase error within the subcarrier loop

Similarly, an expression for the equivalent gain of a subcarrier tracking loop involves integration over all values of both errors:

$$K_{eq}\ (\text{subcarrier}) = \frac{S\,K_1\,K_3}{2\pi\sigma_\theta\sigma_\alpha}\int_{-\infty}^{\infty}\int_{-\infty}^{\infty}\cos\theta\cos\alpha\exp\left\{-\left(\frac{\theta^2}{2\sigma_\theta^2}+\frac{\alpha^2}{2\sigma_\alpha^2}\right)\right\}d\theta d\alpha \qquad (7)$$

where K_1 and K_3 are the gain constants of the balanced modulators BM_1 and BM_3 which constitute the Subcarrier tracking loop.

It must be noted that equations (6) and (7) are identical except for the gain constants $S\,K_2\,K_4$ and $S\,K_1\,K_3$. Furthermore, since the carrier and the subcarrier errors are uncorrelated, the variables can be integrated separately. Thus, if $S\,K_1\,K_3 = S\,K_2\,K_4 = K_0$, integration of these two equations results in an identical expression for the equivalent gain of the error-dependent elements within the loops

$$K_{eq}\ (\text{carrier}) = K_{eq}\ (\text{subcarrier}) = K_0\exp\left\{-\frac{\left(\sigma_\theta^2+\sigma_\alpha^2\right)}{2}\right\} \qquad (8)$$

Equation (8) is important because it shows that the equivalent gain of either loop is determined by the largest of the errors, regardless of the loop where the error is generated.

Based on this expression (Equation (8)) for an equivalent gain of a nonlinear element a linearized model of a two-channel orthogonal demodulator can be constructed. Such a model is shown in Figure 3. As shown there, the two orthogonal loops have been separated into two individual loops with the equivalent gains being determined by the phase errors in both loops.

The next step is to determine the expression for the square of the phase error in each of the two phase-lock loops. Thus, first without considering the effects of cross-coupling, the general expression for the square of the phase error in each phase-lock loop is written as follows:

$$\sigma^2 = \int_0^{\infty} S_m(\omega)\left|1 - H(s)\right|^2 df + \int_0^{\infty}\frac{\exp\left(\sigma^2\right)N_0(\omega)}{2S}\left|H(s)\right|^2 df \qquad (9)$$

where $S_o(\omega)$ and $N_0(\omega)$ are the one-sided power spectral densities of the modulation and noise, respectively, and H(s) is the phase-lock loop transfer function.

In this paper, a second order loop is assumed, and the transfer function used is [8]:

$$H(s) = \frac{S\left(2\zeta\omega_n - \omega_n^2/K\right) + \omega_n^2}{S^2 + 2\zeta\omega_n S + \omega_n} \tag{10A}$$

$$= \frac{\omega_n^2\left[1 + S\left(\frac{2\zeta}{\omega_n} - 1/K\right)\right]}{\omega_n^2 + 2\zeta\omega_n S + S^2} \tag{10B}$$

where ω_n is the natural frequency of the loop in rad/sec, ζ is the loop damping ratio and K is the overall loop gain in sec^{-1}.

For a conventional phase-lock loop preceded by an AGC circuit, the linearized overall loop gain is $SK_L\, e^{-\sigma 2} = K_{eq}$ (1), where (1) indicates a single rather than a cross-coupled coupled loop.

In our case, however, we are considering the effect of the cross-coupling. Thus, to modify (9) to correspond to a case of a dual-loop, orthogonal demodulator, the effect of cross-coupling must be included into the exponential factor on the right hand side of (9). Therefore, one replaces the σ^2 term in the exponent with a $(\sigma_\theta^2 + \sigma_\alpha^2)$ term, the latter being the sum of the single-loop and the cross coupling phase errors.

Additional assumptions which one makes to simplify the integration indicated in (9) are that $N_0(\omega) = N_0$, i.e., constant over the frequency band of interest, and that the FM modulation tracked by either of the loops is Gaussian and its spectrum is such that $S_m(\omega) = S_m$ for $0 \le f \le f_m$ and $S_m(\omega) = 0$ for $f > f_m$. For this type of FM signal the modulation index σ_m is equal to $\sqrt{S_m f_m}$, where f_m is the maximum frequency of modulation. Also, the assumptions that $2\zeta/\omega_n >> 1/K$ and $2\pi f_m/\omega_n << 1$ simplify the integration of (9). Utilizing all of these simplifying assumptions, the general form of (9) after integration in

$$\sigma^2 = \left(\frac{\omega_m}{\omega_{no}}\right)^4 \frac{\sigma_m^2}{5} e^{(\sigma_\theta^2 + \sigma_\alpha^2)} + \frac{N_o\left[1 = 4\zeta_o^2 \exp\left\{-\left(\frac{\sigma_\theta^2 + \sigma_\alpha^2}{2}\right)\right\}\right]\exp\,(\sigma_\theta^2 + \sigma_\alpha^2)}{8\zeta_o S} \tag{11}$$

Equation (11) expresses the total error in each of the loops comprising the orthogonal demodulator. To determine σ^2 for a particular loop one has to substitute the proper values of σ_m ω_m, ω_{no} and ζ_o for that loop.

Equation (11) has several special cases. These are:

1) The error in one of the loops is negligible compared to the error in the companion loop. For this case the orthogonal demodulator behaves as a conventional phaselock loop and not as a Costas demodulator.

2) There is no requirement for modulation tracking for one of the loops. This factor, combined with the narrowing of the corresponding loop, results in an optimum demodulation for Case 1, i.e., that of an information-tracking single phase-lock loop.

and 3) The modulation index, σ_m, and the maximum frequency of deviation, f_m, are equal for both channels of the orthogonal demodulator. For this case the term $(\sigma_\theta^2 + \sigma_\alpha^2)$ in (11) is replaced by $2\sigma^2$.

Orthogonal Demodulator for Two FM Channels - As an example of applying the results shown by (11), we consider an analysis of a two-channel orthogonal demodulator whose purpose is to recover and to separate the frequency modulation information riding on the suppressed carrier and the subcarrier. In other words, at the modulator, one channel modulates the frequency of the carrier and the second channel modulates the frequency of the subcarrier. Finally, the subcarrier is superimposed as the amplitude modulation (suppressed carrier) on the carrier.

At the demodulator end the equations which define the performance of the demodulator are:

$$\sigma^2 = \frac{5\pi \exp\left(-\frac{5\sigma^2}{2}\right)}{32}\sqrt{\frac{\sigma_m}{\sigma}}\left(1 + 4\zeta^2 e^{-\sigma^2}\right)\left(\frac{S}{N}\right)_i^{-1} \tag{12}$$

and

$$\left(\frac{S}{N_o}\right) = \frac{2\sigma_m^2}{\exp(2\sigma^2)}\left(\frac{S}{N}\right)_i \tag{13}$$

where $(S/N)_i$ is the signal-to-noise ratio at the demodulator input and is determined by f_m and σ_m. Equation (12) is derived from (11) by optimization of ω_{no} with respect to the type of modulation used. Equation (13) is the corresponding "FM Improvement Formula" for a quasi-linearized demodulator.

The above-threshold behavior of the second-order dual-channel orthogonal demodulator is described completely by (12) and (13). However, before these equations

can be used to plot the $(S/N)_o$ versus $(S/N)_i$, the region of their validity must be determined. This region is limited to those values of σ which permit each loop to stay phase-locked to the incoming signals despite momentary deviations of the error from the rms value.

The largest value of σ which provides for the "above threshold" operation of each loop and thus makes equations (12) and (13) valid can be determined by first expressing $(S/N)_i$ explicitly in terms of σ and $(S/N)_o$ and then seeking that value which minimizes $(S/N)_i$. Thus, to obtain the required relationship, one eliminates σ_m from both (12) and (13) and solves these for $(S/N)_i$:

$$\left(\frac{S}{N}\right)_i = \frac{\exp\left(\frac{12}{5}\sigma^2\right)}{2\sigma^2}\left[\frac{5\pi\left(1 + 4\zeta_o^2\, e^{-\sigma^2}\right)}{16\zeta_o}\right]^{4/5}\left(\frac{S}{N}\right)_o^{1/5} \tag{14}$$

The σ-dependent factor of Equation (14) is plotted in Figure 4. According to the curve shown in the figure, the minimum value of the σ-dependent factor occurs at σ = 0.74 radian in each of the two loops. Furthermore, according to the curve, those values of σ which exceed 0.74 radian are unstable. This means that at any σ > 0.74 the loop error tends to either settle back to the threshold value of 0.74 radians or to increase without bound, the latter condition corresponding to the loss of tracking. On the other hand, if σ < 0.74 radian, any perturbation will be transient, and the loop error will settle back to the σ value corresponding to a given input signal-to-noise ratio. Therefore, Equations (12) and (13) are valid only in the region $0 < \sigma < 0.74$ radian.

To find the threshold locus for the entire $(S/N)_i$ versus $(S/N)_o$-plane, one substitutes the value of 0.74 radian for σ in Equation (14) :

$$\left(\frac{S}{N}\right)_i = 8.16\left(\frac{S}{N}\right)_o^{1/5} \tag{15}$$

Equation (15) is identical to Equation(24) in [6] except for the factor of 2. Figure 5 provides the comparison between the performance of a single-loop and the dual channel phase-locked demodulator. The two curves shown in the figure were obtained by using Equations (12) (13) and (15) and a similar set of equations for a single loop. The choice of values of σ_m and ζ_o to provide the theoretical prediction of performance was determined by the characteristics of the phase-locked loop available for the experimental evaluation of the demodulator.

From the curves in Figure 5, it is evident that the penalty in $(S/N)_i$ needed to provide some specified quality of output signal is inversely proportional to $(S/N)_o$. For example, at

$(S/N)_o$ = 22 dB, the penalty is about 2 dB while at $(S/N)_o$ = 30 dB this penalty is reduced to about 0.3 dB. However, the maximum penalty which may be paid for the addition of the second channel is equal to 3 dB, i.e., the penalty which corresponds to conventional power division multiplexing.

The increase in penalty is caused by the loss of orthogonality of the two loops at high values of total error σ. In other words, when σ is small the crosstalk between the loops is negligible and each operates as a separate unit. However, as σ increases, the interaction between the loops increases to a point where a 3 dB increase in signal is required to achieve multiplexing.

Experimental Data - Experimental data available on the performance of the orthogonal demodulator provides support for the theoretical considerations presented in the preceding sections of this paper.

The block diagram for the experimental set-up is shown in Figure 6. The modulator/ multiplexer constitutes the transmitter portion of the set-up. The major subunits of this portion are: the subcarrier FM oscillator, the carrier FM oscillator, the balanced amplitude modulator, and the sideband filter. The noise source, the noise attenuator, and the linear combiner simulate the communication channel. The dual-channel demodulator, consisting of carrier and subcarrier tracking loops, simulates the receiver portion of the set-up. The test equipment consists of a noise intensity meter, a distortion analyzer, and a true RMS voltage meter. The test data available can be grouped in the categories listed below.

Threshold Performance Without Modulation - This test measures the relative increase in output noise level versus an equal increase in the IF noise. The purpose of this test is to determine the effect of widening the carrier loop on the performance of the subcarrier channel. Specifically, this test shows the effect of loop cross-coupling due to excessive noise in both of the loops.

For this test an unmodulated carrier signal and a Gaussian noise are mixed linearly and are applied to the input of the demodulator. The signal in this case consists of the two sidebands resulting from the suppressed carrier modulation. However, neither the subcarrier nor the carrier frequency are modulated for this test.

Figure 7 provides a comparison of the theoretical and experimental data.

The performance equivalent to that of a single loop demodulator is simulated by the test setup by narrowing the bandwidth of the carrier loop to about 100 Hz, thus making the contribution due to noise in this loop negligible compared to the noise in the 4 KHz subcarrier loop bandwidth. The noise level is then varied from the level at which a one-to-

one relationship exists between the SNR at the demodulator input and subcarrier loop noise output to that level where this relationship becomes nonlinear, thus indicating the thresholding in the subcarrier loop. Next, the bandwidth of the carrier tracking loop is widened to make it approximately equal to that of the subcarrier channel, i.e., 4 kHz, and the test is repeated. Good agreement, illustrated in Figure 7, is significant because it supports the validity of the quasi-linearized model of a dual channel coherent orthogonal demodulator.

Performance With Simultaneous Frequency Modulation of Subcarrier and Carrier - The second test involves the measurement of the demodulator's threshold performance with sinusoidal modulation applied to the input of both the carrier and the subcarrier channels. Sinusoidal, rather than Gaussian-distributed waveforms are used in this case because of experimental setup limitations. Thus, for the sinusoid tests the frequency of the subcarrier is deviated by ±6 kHz at a 1000 Hz rate. The performance of the orthogonal demodulator is obtained by measuring the output SNR for the subcarrier channel at various SNR's in the input channels. The output SNR is measured by means of a distortion analyzer and a true RMS voltage meter.

Measurements of the subcarrier channel output SNR are performed under the following two conditions: (a) the carrier loop bandwidth narrowed down to about 100 Hz and carrier modulation absent, and (b) carrier loop bandwidth widened to 4 KHz and the carrier frequency deviated by ±6 KHz at the rate of 900 Hz. The first case corresponds to the normal double-sideband operation, with FM on the subcarrier only, and the second case corresponds to a two-channel multiplex mode.

The results corresponding to these conditions are depicted in Figure 8 by curves A and B, respectively. Although the deviation factor used in obtaining these curves does not exactly correspond to $\sigma_m = 3$, i.e., the deviation factor used to plot curves in Figure 5, the similarity between the theoretical and actual performance is striking. Specifically, the near-threshold behavior depicted by the experimental curves corresponds closely to the near-threshold behavior represented by the theoretical curves.

In a similar manner, the performance of the carrier channel can also be tested. Experimental data indicates that this performance agrees within 0.5 dB with the performance of the subcarrier channel.

Conclusions - The theoretical analysis and an experimental evaluation of an orthogonal two-channel demodulator has been presented. This demodulator consists of two cross-coupled phase-lock loops which can track coherently and independently a carrier and a sideband tone. The analysis of the theoretical performance is based on the quasi-linearized model for a two-channel demodulator. The experimental data for such a two-channel

demodulator is in good agreement with the results predicted by the analysis. This agreement supports the validity of the quasi-linearized model for the demodulator.

An applications example is presented where the orthogonal demodulator is used as an efficient demultiplexer for two FM modulated channels. Experimental data taken on such a demodulator/demultiplexer is in agreement with the theoretical performance predictions.

REFERENCES

1) T.P. Costas, "Synchronous Communications," Proc. IRE, Dec. 1956, pp. 1713-1718.

2) W.C. Lindsey and M.K. Simon, Telecommunication Systems Engineering, Prentice Hall, 1973.

3) M.K. Simon and W.C. Lindsey, "Optimum Performance of Suppressed Carrier Receivers with Costas Loop Tracking," IEEE Trans. Communications , COM-25, No. 2, February 1977.

4) K.W. Harris and S. Udalov, "Sideband-Lock SCPDM for Simultaneous Voice and Data Communications," Proceedings of 1977 International Telemetry Conference, Volume XIII, pp. 445-459.

5) R.C. Boonton, Jr., "The Analysis of Nonlinear Control Systems with Random Inputs," reprint of a paper presented at the Symposium on Nonlinear Circuit Analysis, Polytechnic Institute of Brooklyn, April 23-24, 1953.

6) J.A. Develet, Jr., "A Threshold Criterion for Phase-Lock Demodulation," Proc. IEEE, Vol. 51 #2, pp. 349-356, February 1963.

7) J.A. Develet, Jr., "An Analytic Approximation of Phase-Lock Receiver Threshold," IEEE Trans. on Space Electronics and Telemetry, Vol. SET-9 #1, pp. 9-11, March 1963.

8) F.M. Gardner, Phase-lock Techniques, John Wiley & Sons, Inc., 1966.

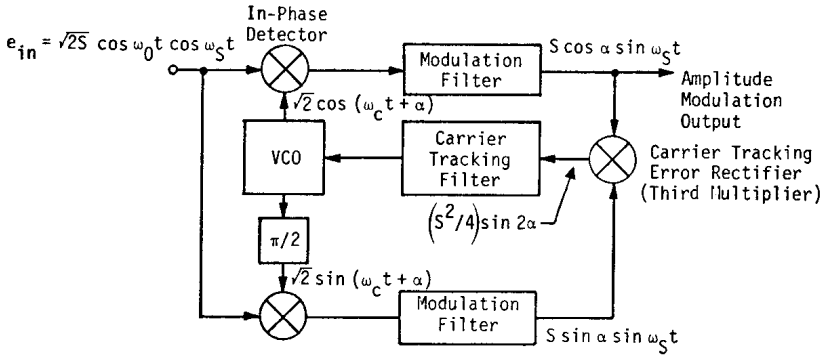

Figure 1. Synchronous Detector Diagram

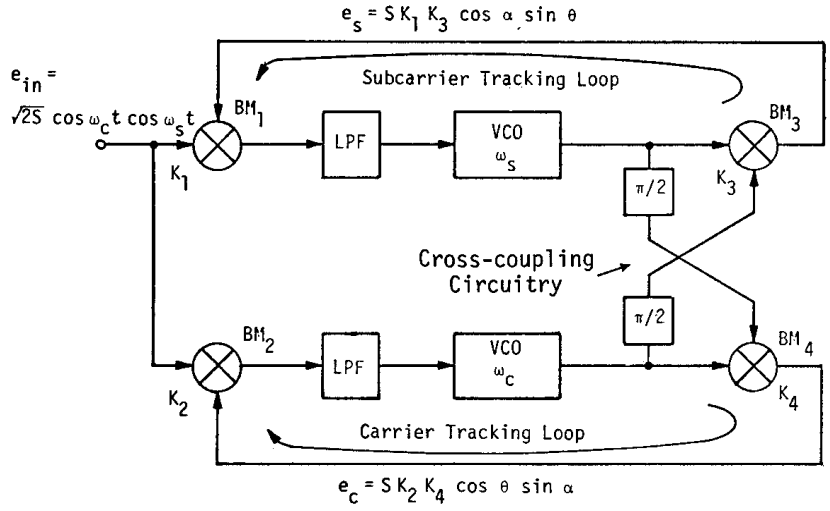

Figure 2. Coherent Demodulator for Orthogonal Sideband and Carrier Tracking

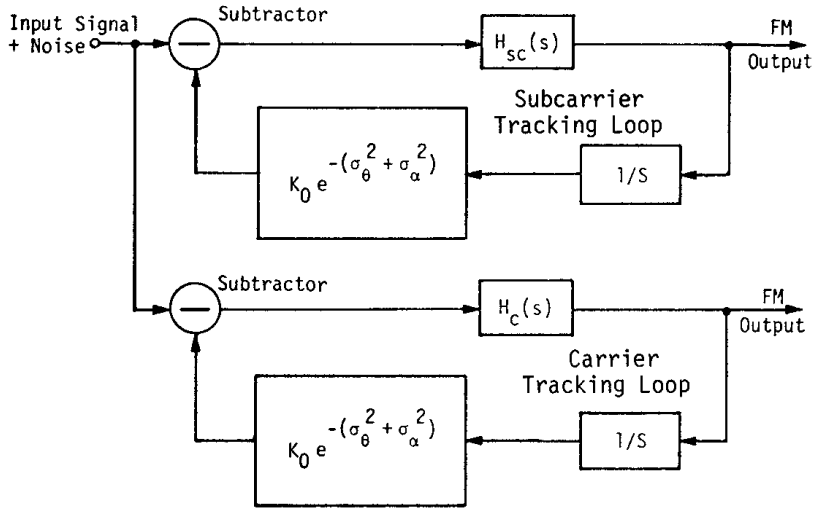

Figure 3. Linearized Block Diagram for a Dual Channel Orthogonal Demodulator

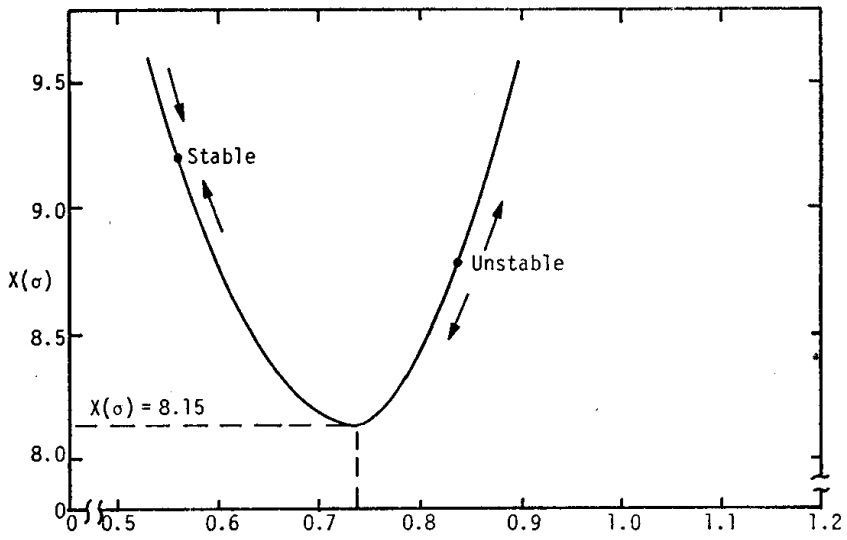

Figure 4. Plot of X(σ) vs. σ for a Dual Loop Orthogonal Demodulator

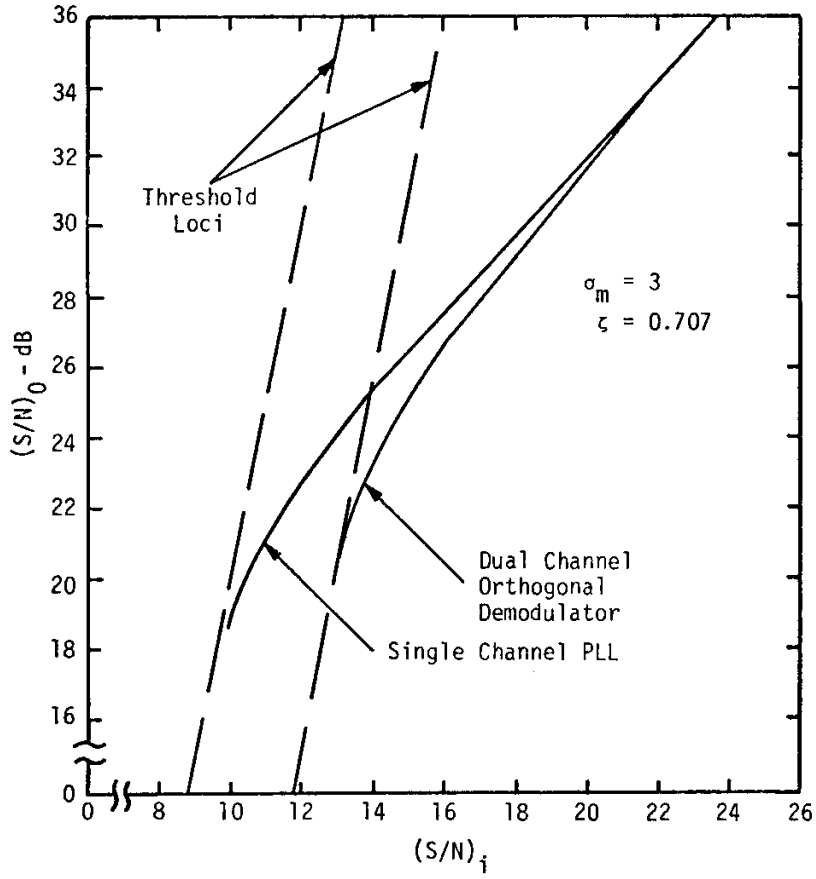

Figure 5. Threshold Performance Comparison of Orthogonal Demodulator and PLL

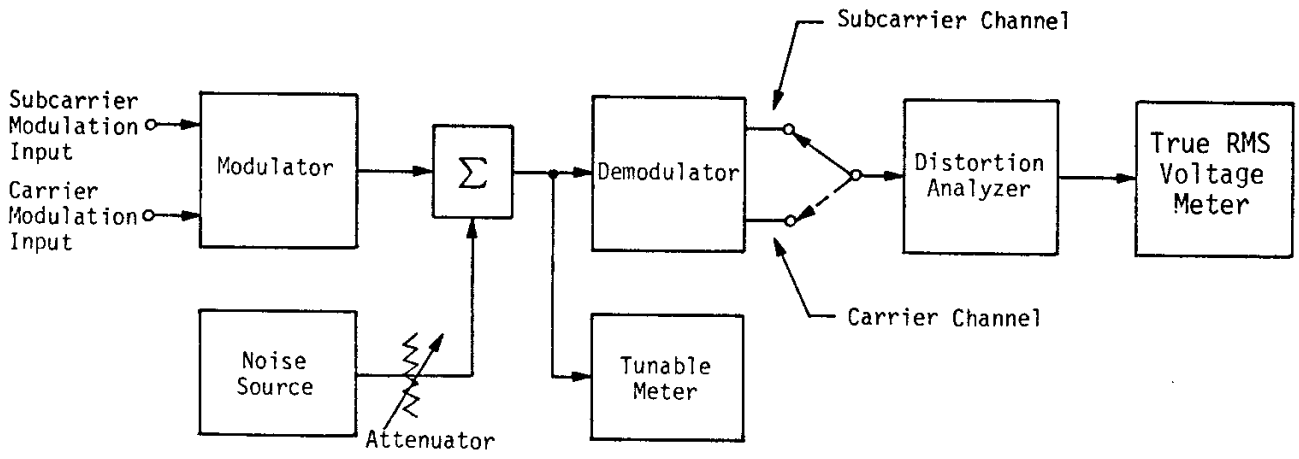

Figure 6. Coherent Orthogonal Demodulator Test Setup

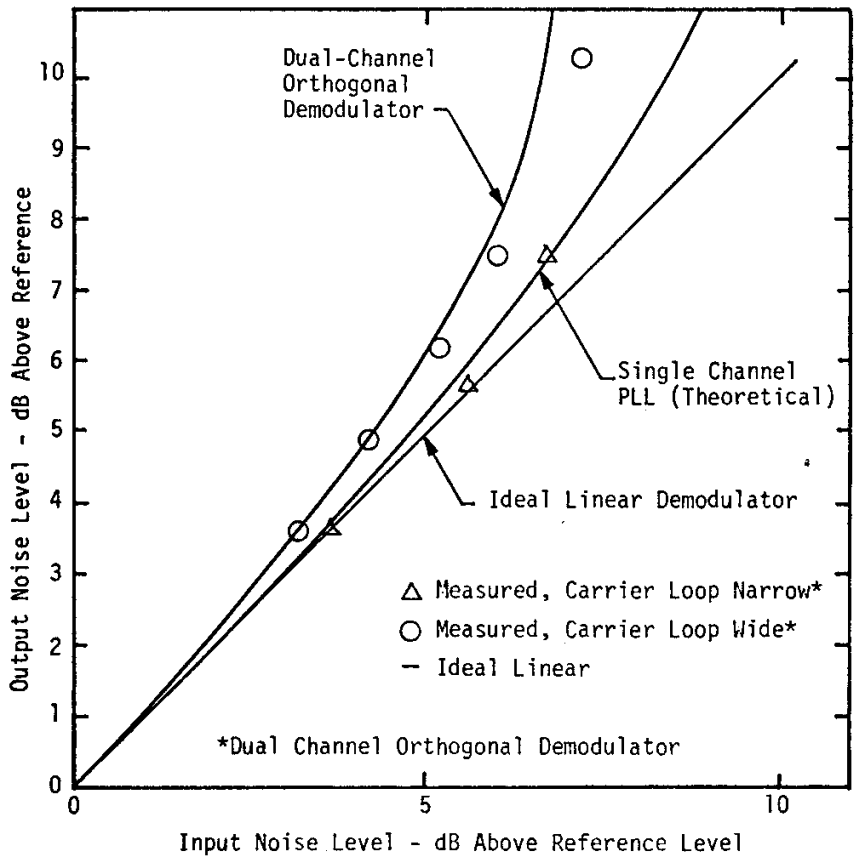

Figure 7. Increase in Output Noise Level for the Orthogonal Demodulator vs. Single Channel PLL

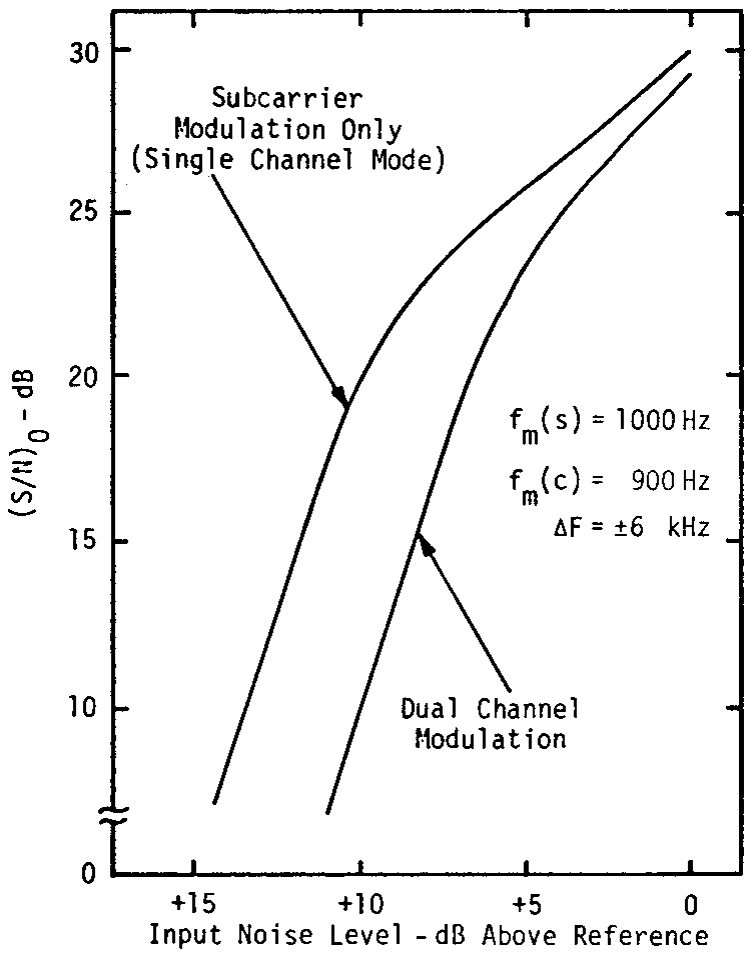

Figure 8. Threshold Performance of the Orthogonal Demodulator for Single and Dual Channel Modes